12th International Symposium on Turbulence and Shear Flow Phenomena (TSFP12)
Osaka, Japan, July 19–22, 2022

TURBULENCE ENHANCEMENT IN BODY FORCE OPPOSED FLOWS

Stephen D Jackson
Department of mechanical engineering
University of Sheffield
Sir Fredrick Mappin Building, Mappin Street, S1 3JD
sdjackson1@sheffield.ac.uk

Shuisheng He
Department of mechanical engineering
University of Sheffield
Sir Fredrick Mappin Building, Mappin Street, S1 3JD
s.he@sheffield.ac.uk

ABSTRACT

Turbulence in vertical pipe flows changes strongly when influenced by non-uniform body forces. A motivating example is buoyancy acting in mixed convection flows. Here we run Direct Numerical Simulations (DNSs) of flows subjected to a set of idealised streamwise body forces opposing the main flow direction. By systematically varying body force profile shape we report the resulting changes to turbulence characteristics and coherent structures. The conventional understanding is that by introducing an opposing non-uniform body force whilst maintaining an Equal Flow Rate (EFR), turbulence will increase. Here we show that by instead maintaining an Equal Pressure Gradient (EPG), the key turbulence characteristics do not change. As a result the increased turbulence observed in the conventional theory can be explained by an increased 'apparent Reynolds number'. On top of this we show how the turbulent shear stress, and velocity profiles can be easily predicted simply from the non-uniform body force profile and EPG reference data despite the non-equilibrium nature of the flows.

INTRODUCTION

The use of non-uniform body forces, while initially seeming abstract, is a useful generalisation since it can underpin various physical phenomena. For example there are flow control techniques, such as Kühnen *et al.* (2018) who applied pseudo body forces with streamwise fluid injection in order to force flow laminarisation. Other examples using actual body forces occur frequently in magnetohydrodynamics and mixed convection. Here we focus our attention on opposing non-uniform body forces which act against the main flow direction, causing increased turbulence. This is particularly important in mixed convection cooling systems where the changes in turbulence may lead to heat transfer enhancement or deterioration. In particular Hall & Jackson (1969), proposed that the buoyancy causes a redistribution of the shear stress, and in the buoyancy aided case the shear stress may be reduced to zero in the near-wall region which causes strong laminarisation whilst the shear is increased in the buoyancy opposed case leading to stronger turbulence. Here we aim to provide a new perspective on the mechanism by which turbulence is increased. Petukhov *et al.* (1988) showed that the effect of buoyancy can be split into two parts, the external (indirect) effect where the change in density causes a change to the mean velocity profile which in turn leads to a change in turbulence production, and the structural (direct) effect where density fluctuations directly cause velocity fluctuations. Here we choose to investigate only the direct effect. In conjunction with the Boussinesq approximation these conditions allows the use of idealised body force profiles.

METHODOLOGY

The DNSs are conducted using an in-house Fortran code CHAPSim (Seddighi-Moornani (2011), He & Seddighi (2013)) which uses a fractional step method with a second order central difference scheme for the spatial discritisation. The temporal terms are discritised with an explicit third order Runge-Kutta scheme for the non-linear terms, and an implicit Crank-Nicholson scheme for the linear terms. All cases use a pipe flow domain of length $20R$ where R is the pipe radius.

The non-uniform streamwise body force profiles are chosen based on physical density profiles, with linear profiles for flows at sub-critical pressure (Groups A and B), and step change profiles for those at supercritical pressure (Group C) which show sudden strong density changes across the pseudo-critical temperature (Figure 1). We non-dimensionalise using the radius R^*, bulk velocity U_b^*, density ρ^*, and viscosity μ^* so that $Re = \frac{\rho^* U_b^* R^*}{\mu^*}$, $f = \frac{f^* R^*}{\rho^* U_b^{*2}}$, $P = \frac{2P^*}{\rho^* U_b^{*2}}$.

The body force profiles are chosen such that groups A and C have increasing coverage, which is to say that the body force acts further into the pipe, whereas group B has an increasing amplitude at the wall. In general all the cases have a base Reynolds number of 2650, with the exception being case $L2$ which has a lower base Reynolds number of 1000, but the same profile shape as case $B2$. We also use three physical profiles $P1-P3$ extracted from You *et al.* (2003) temperature profiles, hence decoupling the flow and thermal fields and thus only considering the indirect effect. In order to determine the strength of each body force profile, we use the integral,

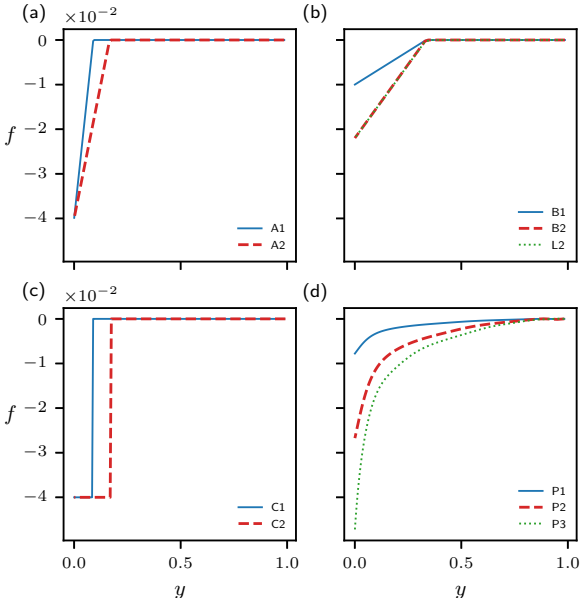

Figure 1. Opposing non-uniform body force profiles .

Table 1. DNS case table.

Case	$Re_{\tau p}$	Re_τ	F
EFR reference	180	180	0
A1, A2	201-229	169-174	0.0035-0.0063
B1, B2	208-237	181-182	0.0029-0.0066
C1, C2	230-277	113-182	0.0066-0.013
P1, P3	198-260	174-180	0.002-0.011
L2	94.6	75.347	0.0066

$F = 2\int_0^1 rf\,dr$ as shown in Table 1.

Here we extend the approach of He *et al.* (2016) for flow laminarisation to explain turbuence enhancement. That is, we use an alternative perspective where the body force influenced flows are compared to their equal pressure gradient reference flows rather than their equal flow rate reference flows. In order to compare flow characteristics in this framework, we use an alternative scaling similar to the inner scaling, however while the usual wall scaling is based upon the wall shear stress, τ_w, we instead use the wall shear stress of the EPG flow (or equivalently the pressure gradient of the flow concerned), τ_{wp} and denote this using a "+1" notation such that

$$y^{+1} = \frac{y}{\nu}\sqrt{\frac{\tau_{wp}}{\rho}}.$$

This perspective has proved useful in various studies building on the analysis in He *et al.* (2016). For example a detailed analysis of the laminarisation mechanisms for supercritical heated pipe flows using pseudo-body forces from He *et al.* (2021). While Marensi *et al.* (2021) shows how the new perspective can also give new insight in the critical Reynolds number for transition / reverse transition in comparison with linear stability analysis.

RESULTS

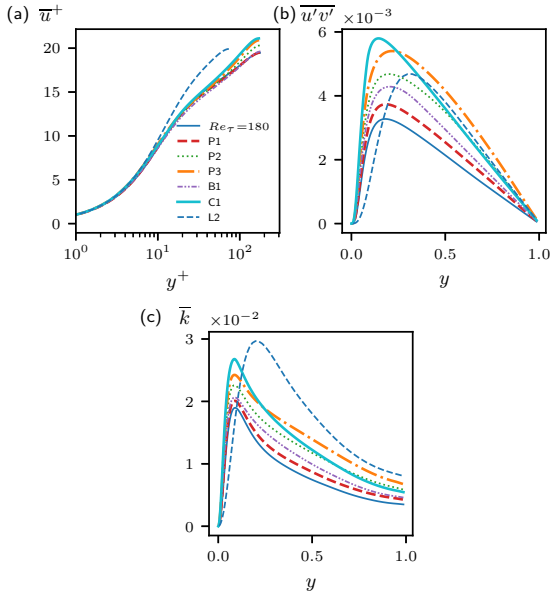

Figure 2. Velocity profiles, Turbulent shear stress and Turbulent kinetic energy for various cases.

We first show a brief overview of how turbulence characteristics change with different body force profiles. The velocity profiles (Figure 2a) change mildly, with increasing centerline velocity and reduced near wall velocity with the exception of very low coverage cases such as $A1$. Turbulence Shear Stress (TSS) in Figure 2b and Turbulence Kinetic Energy (TKE) in Figure 2c show strong increases with increasing body force strength. Essentially from the conventional viewpoint turbulence increases, which is inline with previous studies.

By comparing the eddy viscosity profiles (Figure 3) we see from the conventional viewpoint (left) the eddy viscosity increases with stronger body forces, which is to be expected since turbulence should be increasing. However, from the alternative perspective (right), the eddy viscosity profiles collapse, except the case $L2$ which has the lower base Reynolds number. Even still, the eddy viscosity profiles are virtually the same as their EPG reference flows, particularly in the near wall region as indicated in the plot. (Here only the EPG flows for cases $L2$, $A1$, and $C2$ are shown for simplicity, however agreement is strong for all cases).

More than this, Figure 4 shows the RMS fluctuations in each direction using the standard scaling (a, c), and the alternative EPG scaling (b, d). In the usual scaling and compared to their EFR reference case, the addition of the body force causes increased turbulence in all directions. (the spanwise fluctuations act similarly to the wall normal fluctuations and so have been ommitted from the plot, although sometimes still discussed) There is a small increase of 14% in the streamwise direction but a much larger increase of 41% and 50% in the wall normal and spanwise directions respectively for the strongest case $P3$. The fact that the changes to v' and w' are stronger than u' suggests that opposing body forces cause the flow to

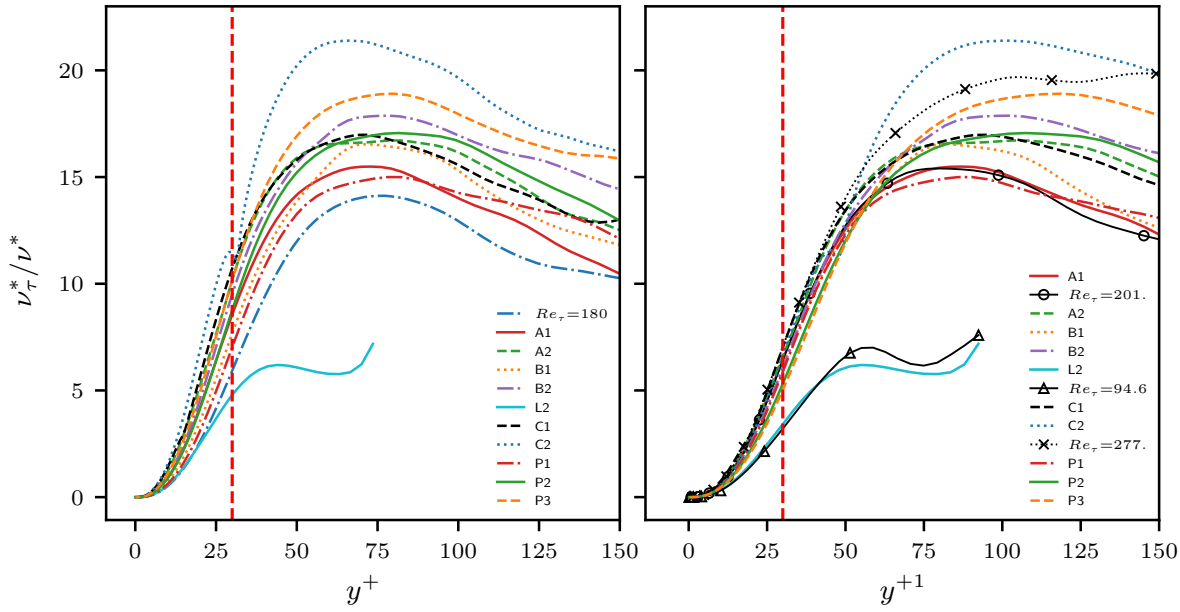

Figure 3. Eddy viscosity plotted against y scaled by standard inner scaling (left) and EPG scaling (right).

become more isotropic. The behaviour is different in the EPG framework, there is very little change to the v' and w' fluctuations. For cases $P2$ and $P3$, which have strong coverage, there is a slight reduction of around 12%. These are particularly significant fluctuations in relation to turbulent mixing and hence heat transfer. In general this means that the turbulence in body force opposed flows tends to act the same as their EPG flows, and hence can be thought of as acting according to an apparent Reynolds number which is the Reynolds number of its EPG flow ($Re_{\tau p}$ in Table 1). Interestingly, comparing case $B2$ to $L2$, which have the same non-dimensional body force, but $L2$ has a lower Reynolds number there is a much smaller reduction in the streamwise velocity fluctuations. This suggests that for lower Reynolds number flows there is less deviation away from its corresponding EPG flow.

The behaviour of the RMS fluctuations can be explained using the Reynolds stress budgets. Using case $A2$ as an example, Figure 5a shows the streamwise Reynolds stress budgets in the conventional scaling. As body forces are imposed, the production term (I) increases as more energy is provided to the streamwise fluctuations. The pressure strain term (IV) also strongly increases as streamwise streaks break down into v' and w' fluctuations and this acts as an energy source for wall normal fluctuations, increasing all wall normal budget terms as shown in Figure 5c. This is also related to the increased v' fluctuations in Figure 4c. The story is different in the EPG framework. The production decreases, representing a reduction in the energy contained in the streamwise fluctuations. However the key point is that the pressure strain term is exactly the same suggesting that the body force does not change how the energy is transferred from streamwise fluctuations into the wall normal and spanwise components. This is shown to be related to a weakening of the streaks, but no significant changes in streak breakdown. While only case $A2$ is shown here, the same behaviour is observed in all cases with a low coverage. For rare cases with a larger coverage, such as $P2$ and $P3$ the pressure strain is slightly reduced, corresponding with the behaviour of the fluctuations in Figure 4d, however it is interesting to note that the eddy viscosity profiles still show good agreement.

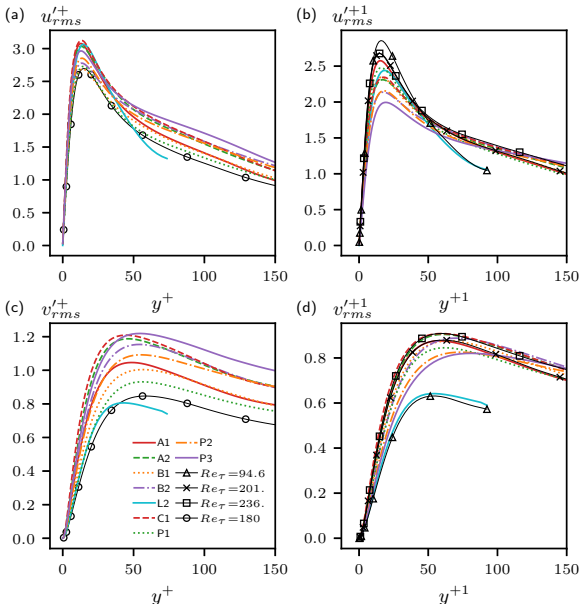

Figure 4. Root mean square turbulent fluctuations plotted in standard inner scaling ((a) & (c)), and EPG scaling ((b), (d)).

Streaks

In Figure 6 we show correlations of fluctuating velocities in the streamwise and spanwise directions, with the aim to characterise the streak length and spacing. Figures 6a and b show the spanwise correlations with the minimum points indicated by the markers. In the conventional scaling the streak

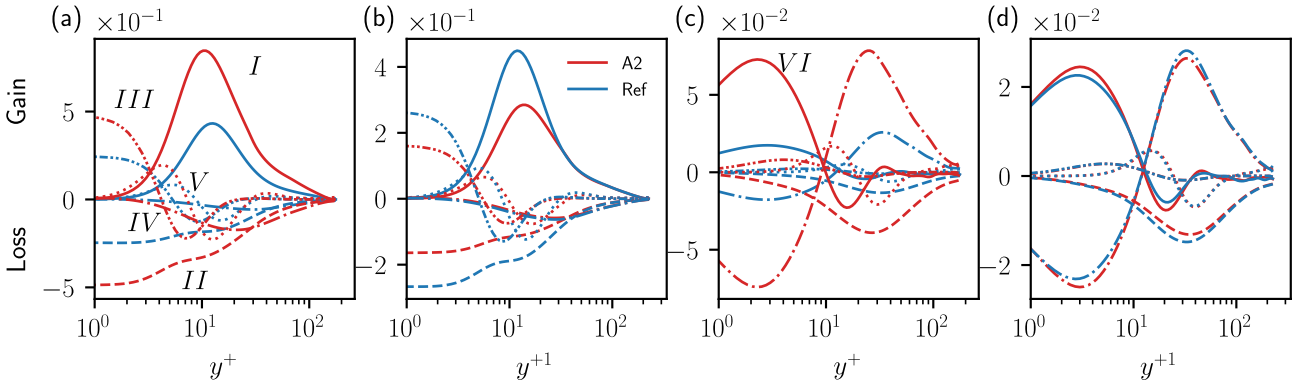

Figure 5. Reynolds stress budget terms in the streamwise direction (a, b), and the wall normal direction (c, d). The terms shown are Production (*I*), Dissipation (*II*), Viscous Diffusion (*III*), Pressure Strain (*IV*), Turbulent Transport (*V*), and Pressure Diffusion (*VI*). The reference flow is EFR in plots with conventional '+' scaling and EPG in the '+1' scaling.

spacing reduces by $\delta(r\theta)^+ \approx 20$ compared to their EFR reference flow due to the effect of the body force. On the other hand, in the new scaling the flows the spacings are in general more clustered and agree better with their EPG flows. For the streamwise correlations, Figure 6c shows how the body force influenced flows become less correlated in a shorter streamwise distance. This, in conjunction with the increased pressure strain and enhanced v' and w' fluctuations strongly suggests that the body forces cause stronger streak breakdown. However, using the alternative scaling in Figure 6d the streamwise correlations collapse to each other and show very little shortening of the streaks compared to their EPG flow. In this sense it is as if the streaks in the body force influence flow have the same structure as that of their corresponding EPG flow. However, taking into account the reduction in u' in Figure 4b, the conclusion is that the streaks become weakened (note the reduced production), however maintain the same structure as their EPG flow.

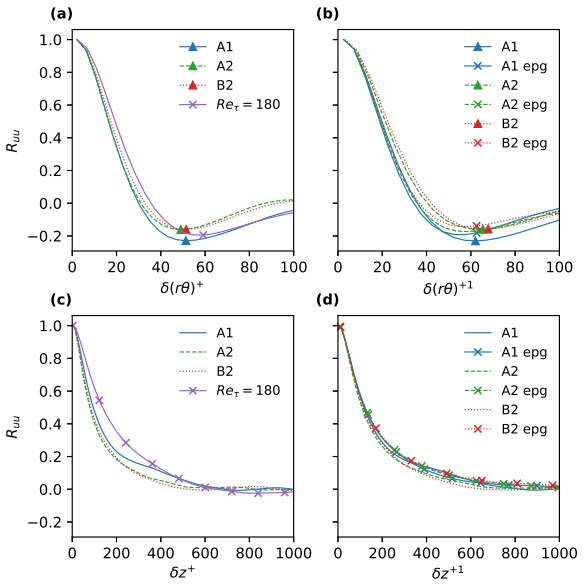

Figure 6. Spanwise and streamwise correlations taken at a wall normal distance of $y^{+(1)} = 12$. Markers in (a) and (b) indicate the minimum point.

Predictions

By using the fact that whilst maintaining constant pressure gradient the eddy viscosity is unchanged by the addition of a body force ($\nu_t = \nu_{tp}$), where subscript p denotes that it is corresponding to the EPG flow, the turbulent shear stress and the velocity profiles can be predicted simply from the EPG reference flow, and the body force profile. Following the method from He *et al.* (2016), the body force influenced RANS flow, can be written as,

$$0 = \left(-\frac{\mathrm{d}P}{\mathrm{d}x}\right)_p + \frac{1}{r}\frac{\partial}{\partial r}\left[r\left(\frac{1}{Re}\frac{\partial \overline{u}_z}{\partial r} - \overline{u_z' u_r'}\right)\right] + f. \quad (1)$$

The total flow can be split into its EPG flow, which is often easily available from reference data

$$0 = \left(-\frac{\mathrm{d}P}{\mathrm{d}x}\right)_p + \frac{1}{r}\frac{\partial}{\partial r}\left[r\left(\frac{1}{Re}\frac{\partial (\overline{u}_z)_p}{\partial r} - (\overline{u_z' u_r'})_p\right)\right] \quad (2)$$

and a perturbation flow which is simply the difference between the body force influenced flow (1) and EPG flow (2). Noting if one applies the eddy viscosity hypothesis $\left(\overline{u_z' u_r'} = -\frac{\nu_t}{Re}\frac{\partial \overline{u}_z}{\partial r}\right)$ and using the fact that the pressure gradient and eddy viscosity are the same between the two flows ($\nu_t = \nu_{tp}$), the perturbation flow can be written as (1) - (2),

$$0 = \frac{1}{r}\frac{\partial}{\partial r}\left[r\left(\frac{1}{Re}\frac{\partial (\overline{u}_z)_b}{\partial r} + \frac{\nu_{tp}}{Re}\frac{\partial (\overline{u}_z)_b}{\partial r}\right)\right] + f. \quad (3)$$

The subscript b is used to represent the perturbation such that $(\overline{u_z' u_r'})_b = \overline{u_z' u_r'} - (\overline{u_z' u_r'})_p$ and $(\overline{u_z})_b = \overline{u_z} - (\overline{u_z})_p$. By solving Equation 3 one can obtain $(\overline{u_z' u_r'})_b$ and $(\overline{u_z})_b$, which when combined with the EPG reference flow can be used to solve for the total flow.

Figure 7 shows profiles of the turbulent shear stress. In the usual inner scaling the shear stress increases highlighting the non-equillibrium nature of the flows which are typically difficult to predict. However by using these new ideas the turbulent shear stress of the idealised profiles can be predicted very well (Figure 7a). The physical cases $P1 - P3$ are also shown to have excellent predictions, and the shear stress profiles from You *et al.* (2003) are also included. In these cases the flow and energy equations are coupled and the direct effect

is considered. Since the profiles are close, this lends weight to the idea that the indirect effect dominates in these flows.

Next we use FIK expression introduced by Fukagata *et al.* (2002) to determine different dynamical contributions to the skin friction, in particular the laminar contributions and turbulent contributions split into the EPG and perturbation flows using the decomposition $\overline{u_z'u_r'} = (\overline{u_z'u_r'})_b + (\overline{u_z'u_r'})_p$. This gives the following terms:

$$C_f = \underbrace{\frac{16}{Re}}_{i} + \underbrace{16\int_0^1 2r^2(\overline{u_r'u_z'})_p\,dr}_{ii} + \underbrace{16\int_0^1 2r^2(\overline{u_r'u_z'})_b\,dr}_{iii} + \underbrace{16\int_0^1 (r^2-1)(f-F)r\,dr}_{iv}$$

These terms represent different physical contributions, terms *i* & *iv* represent the laminar contributions, while terms *ii* and & *iii* are the turbulent contributions from the EPG and perturbation flows respectively, the contributions are shown in Figure 7c. The term *i* does not change between cases, since they are considered in the EFR framework and have the same Reynolds number. However each case individually has a different EPG flow and hence different apparent Reynolds numbers. This is linked to the change in term *ii* where the turbulence shear stress of the EPG flow, $(\overline{u_r'u_z'})_p$, is changed due to the EPG acting at a different Reynolds number. By using the predicted turbulent shear stress shown above, we obtain a prediction of term *iii*, and hence a prediction of C_f. This is shown in Figure 7c (grey dot), agreeing very strongly with the actual DNS values of C_f (black cross).

It should be noted that the body force influenced flow does not act exactly like its EPG reference flow. The effect of the body force clearly reduces the streamwise fluctuations, (Figure 4 (d)) which is thought to have links to some aspects of the coherent structures, namely a weakening of the streamwise streaks. Importantly though, this change does not influence the turbulence mixing of the flow. Interestingly, comparing case *B*2 to *L*2, which have the same non-dimensional body force, but *L*2 has a lower Reynolds number there is a much smaller reduction in the streamwise velocity fluctuations. This suggests that for lower Reynolds number flows there is less deviation away from its corresponding EPG flow.

CONCLUSIONS

- Flows influenced by opposing non-uniform body forces have much stronger turbulence characteristics, including eddy viscosity, turbulent shear stress, turbulent kinetic energy. Turbulence also becomes more isotropic.
- In contrast, when the pressure gradient is kept constant, as opposed to the flow rate (used in bullet point 1), the additional body force does not change the key turbulence characteristics.
- The increase in turbulence in the conventional understanding can be explained using an apparent Reynolds number, which is the Reynolds number of its EPG reference flow.
- Streak breakdown is not enhanced by applying body forces whilst maintaining a constant pressure gradient.
- By exploiting the unchanging eddy viscosity, usually difficult to predict quantities such as turbulent shear stress, velocity profiles and skin friction can be predicted well simply from reference data and a given body force profile.

Acknowledgements

This work makes use of DNS code CHAPSim, which is currently maintained by CCP-NTH (EP/T026685/1). Also grateful acknowledgments to Dr W.Wang for insights into CHAPSim and to M. Falcone and Dr K. Chinembiri for many useful discussions.

REFERENCES

Fukagata, Koji, Iwamoto, Kaoru & Kasagi, Nobuhide 2002 Contribution of Reynolds stress distribution to the skin friction in wall-bounded flows. *Physics of Fluids* **14** (11), L73–L76.

Hall, WB & Jackson, JD 1969 Laminarization of a turbulent pipe flow by buoyancy forces. *ASME-AMER SOC MECHANICAL ENG* .

He, J., Tian, R., Jiang, P.X. & He, S. 2021 Turbulence in a heated pipe at supercritical pressure. *Journal of Fluid Mechanics* **920**, A45.

He, S., He, K. & Seddighi, M. 2016 Laminarisation of flow at low Reynolds number due to streamwise body force. *Journal of Fluid Mechanics* **809**, 31–71.

He, S. & Seddighi, M. 2013 Turbulence in transient channel flow. *Journal of Fluid Mechanics* **715**, 60–102.

Kühnen, Jakob, Song, Baofang, Scarselli, Davide, Budanur, Nazmi Burak, Riedl, Michael, Willis, Ashley P., Avila, Marc & Hof, Björn 2018 Destabilizing turbulence in pipe flow. *Nature Physics* **14** (4), 386–390, publisher: Springer US.

Marensi, Elena, He, Shuisheng & Willis, Ashley P. 2021 Suppression of turbulence and travelling waves in a vertical heated pipe. *Journal of Fluid Mechanics* **919**, A17.

Petukhov, BS, Polyakov, AF & Launder, BE 1988 Heat transfer in turbulent mixed convection .

Seddighi-Moornani, Mehdi 2011 Study of Turbulence and Wall Shear Stress in Unsteady Flow over Smooth and Rough Surfaces p. 236.

You, Jongwoo, Yoo, Jung Y. & Choi, Haecheon 2003 Direct numerical simulation of heated vertical air flows in fully developed turbulent mixed convection. *International Journal of Heat and Mass Transfer* **46** (9), 1613–1627.

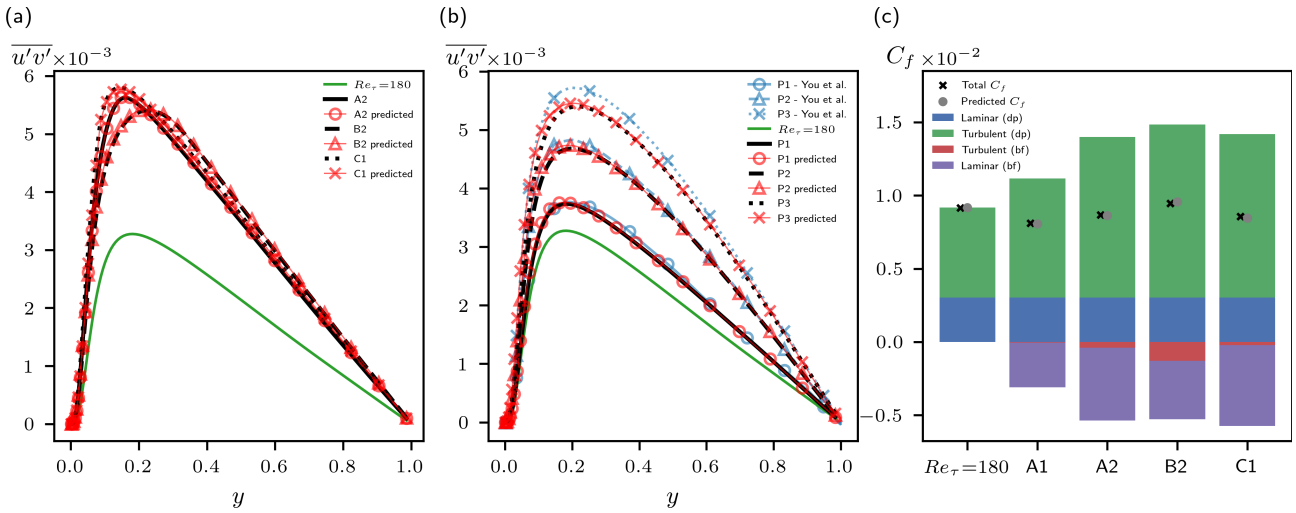

Figure 7. Turbulent shear stress profiles and skin friction with their predictions calculated using EPG reference data.